Ghost-surfaces and island detection.

S.R.Hudson

Abstract

1. Various routines for
   1. constructing quadratic-flux minimizing surfaces & ghost surfaces,
   2. estimating island widths,
   3. locating the homoclinic tangle, homoclinic points,
   4. identifying the last closed flux surface,
   5. locating cantori, flux across cantori,
   6. almost straight fieldline coordinates for arbitrary, non-integrable fields,

   have now been incorporated into HINT2, SPEC (of course), M3D-C_1, . . .

This poster is online at http://w3.pppl.gov/~shudson/Papers/Conference/2015Sherwood/Hudson2015SherwoodCEMM.pdf

Classical Mechanics 101:

The action integral is a functional of a curve in phase space.

1. The action, S, is the line integral along an arbitrary "trial" curve $\{\mathcal{C} : q \equiv q(t)\}$, of the Lagrangian,

$$\mathcal{L} \equiv \underbrace{T(\dot{q}, q)}_{\text{kinetic}} - \underbrace{U(q,t)}_{\text{potential}}, \quad S \equiv \int_{\mathcal{C}} \mathcal{L}(q, \dot{q}, t) dt$$

2. For magnetic fields, $\mathbf{B}$, the action is the line integral, of the vector potential, $\mathbf{B} = \nabla \times \mathbf{A}$,

$$S \equiv \int_{\mathcal{C}} \mathbf{A} \cdot d\mathbf{l}, \ \text{ along } \{\mathcal{C} : \theta \equiv \theta(\zeta), \rho \equiv \rho(\theta)\}.$$

3. Physical trajectories (magnetic fieldlines) extremize the action:

$$\delta S = \int_{\mathcal{C}} d\zeta \left(\delta\theta \frac{\partial S}{\partial \theta} + \delta\rho \frac{\partial S}{\partial \rho} \right), \text{ where } \boxed{\frac{\partial S}{\partial \theta} \equiv \sqrt{g} B^{\rho} - \dot{\rho} \sqrt{g} B^{\zeta}} \text{ and } \boxed{\frac{\partial S}{\partial \rho} \equiv \dot{\theta} \sqrt{g} B^{\zeta} - \sqrt{g} B^{\theta}}.$$

extremal curves satisfy $\dot{\rho} = B^{\rho}/B^{\zeta}$, and $\dot{\theta} = B^{\theta}/B^{\zeta}$.

4. Action-extremizing, periodic curves may be minimizing or minimax.

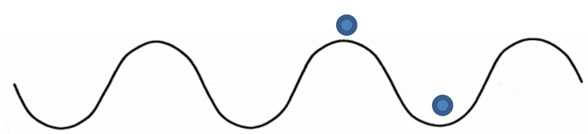

5. Ghost surfaces are defined by an action-gradient flow between the minimax and minimizing periodic orbit.

Ghost surfaces, a class of almost-invariant surface, are defined by an action-gradient flow between the action minimax and minimizing fieldline.

1. Action, $S[\mathcal{C}] \equiv \int_{\mathcal{C}} \mathbf{A} \cdot d\mathbf{l}$, and action gradient, $\dfrac{\partial S}{\partial \theta} \equiv \sqrt{g} B^{\rho} - \dot{\rho} B^{\zeta}$.

2. Enforce $\dfrac{\partial S}{\partial \rho} \equiv \dot{\theta} B^{\zeta} - \sqrt{g} B^{\theta} = 0$, i.e. invert $\dot{\theta} \equiv B^{\theta}/B^{\zeta}$ to obtain $\rho = \rho(\dot{\theta}, \theta, \zeta)$; so that trial curve is completely described by $\theta(\zeta)$, and the action reduces from $S \equiv S[\rho(\zeta), \theta(\zeta)]$ to $S \equiv S[\theta(\zeta)]$

3. Define action-gradient flow: $\boxed{\dfrac{\partial \theta(\zeta;\tau)}{\partial \tau} \equiv -\dfrac{\partial S[\theta]}{\partial \theta}}$, where τ is an arbitrary integration parameter.

4. Ghost-surfaces are constructed as follows:

   i. Begin at action-minimax ("O", "not-always-stable") periodic fieldline, which is a saddle;
   ii. initialize integration in decreasing direction (given by negative eigenvalue/vector of Hessian);
   iii. the entire curve "flows" down the action gradient, $\partial_{\tau}\theta = -\partial_{\theta} S$;
   iv. action is decreasing, $\partial_{\tau} S < 0$;
   v. finish at action-minimizing ("X", unstable) periodic fieldline.
   vi. ghost surface described by $\mathbf{x}(\zeta, \tau)$, where τ is a fieldline label.

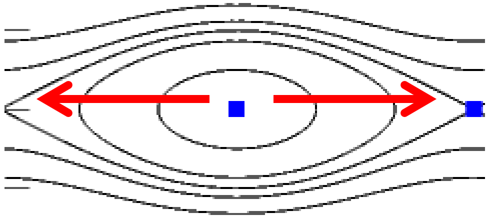

The construction of extremizing **curves** of the **action** generalized extremizing **surfaces** of the **quadratic-flux**

1. $\delta S = \int_{\mathcal{C}} d\zeta \left(\delta\theta \frac{\partial S}{\partial \theta} + \delta\rho \frac{\partial S}{\partial \rho} \right)$, where $\boxed{\frac{\partial S}{\partial \theta} \equiv \sqrt{g} B^\rho - \dot{\rho} \sqrt{g} B^\zeta}$ and $\boxed{\frac{\partial S}{\partial \rho} \equiv \dot{\theta} \sqrt{g} B^\zeta - \sqrt{g} B^\theta}$.
2. Extremal curves satisfy $\frac{\partial S}{\partial \theta} = 0$, i.e. $\dot{\rho} = B^\rho / B^\zeta$, and $\frac{\partial S}{\partial \rho} = 0$, i.e. $\dot{\theta} = B^\theta / B^\zeta$.
3. Introduce toroidal surface, $\rho \equiv P(\theta, \zeta)$, and *family* of angle curves, $\theta_\alpha(\zeta) \equiv \alpha + p\,\zeta/q + \tilde{\theta}(\zeta)$, where α is a fieldline label; p and q are integers that determine periodicity; and $\tilde{\theta}(0) = \tilde{\theta}(2\pi q) = 0$.
4. On *each* curve, $\rho_\alpha(\zeta) = P(\theta_\alpha(\zeta), \zeta)$ and $\theta_\alpha(\zeta)$, can <u>enforce</u> $\frac{\partial S}{\partial \rho} = 0$; generally $\nu \equiv \frac{\partial S}{\partial \theta} \neq 0$.
5. The *pseudo* surface dynamics is defined by $\dot{\theta} \equiv B^\theta / B^\zeta$ and $\dot{\rho} \equiv \partial_\theta P\, \dot{\theta} + \partial_\zeta P$.
6. Corresponding *pseudo* field $\mathbf{B}_\nu \equiv \dot{\rho}\, B^\zeta\, \mathbf{e}_\rho + \dot{\theta}\, B^\zeta\, \mathbf{e}_\theta + B^\zeta \mathbf{e}_\zeta$; simplifies to $\mathbf{B}_\nu = \mathbf{B} - \frac{\nu}{\sqrt{g}}\, \mathbf{e}_\rho$.
7. Introduce the <u>**quadratic-flux functional**</u>: $\boxed{\varphi_2 \equiv \frac{1}{2} \iint d\theta d\zeta \left(\frac{\partial S}{\partial \theta} \right)^2}$
8. Allowing for δP, the first variation is $\delta\varphi_2 = \iint d\theta d\zeta\ \delta P\ \sqrt{g}\ \underbrace{\left(B^\theta \partial_\theta + B^\zeta \partial_\zeta \right) \nu}_{\text{Euler-Lagrange for QFMs}}$.

Alternative Lagrangian integration construction:
QFM surfaces are families of extremal curves of the constrained-area action integral.

1. Introduce $F(\boldsymbol{\rho}, \boldsymbol{\theta}) \equiv \int_{\mathcal{C}} \mathbf{A} \cdot d\mathbf{l} - \nu \left(\int_{\mathcal{C}} \theta \nabla \zeta \cdot d\mathbf{l} - a \right)$, where $\boldsymbol{\rho} \equiv \{\rho_i\}$, $\boldsymbol{\theta} \equiv \{\theta_i\}$;
   where ν is a Lagrange multiplier, and a is the required "area", $\int_0^{2\pi q} \theta(\zeta)\, d\zeta$.

2. An identity of vector calculus gives $\delta F = \int_{\mathcal{C}} d\mathbf{l} \times (\nabla \times \mathbf{A} - \nu \nabla\theta \times \nabla\zeta) \cdot \delta\mathbf{l}$,
   extremizing curves are tangential to $\mathbf{B} - \nu \nabla\theta \times \nabla\zeta = \mathbf{B} - \frac{\nu}{\sqrt{g}} \mathbf{e}_\rho = \mathbf{B}_\nu$.

3. Constrained-area action-extremizing curves satisfy $\frac{\partial F}{\partial \rho_i} = 0$ and $\frac{\partial F}{\partial \theta_i} = 0$.

4. The piecewise-constant representation for $\rho(\zeta)$ and $\partial_{\rho_i} F = 0$ yields $\rho_i = \rho_i(\theta_{i-1}, \theta_i)$, so the trial curve is completely described by θ_i, i.e. $F \equiv F(\boldsymbol{\theta})$.

5. The piecewise-linear representation for $\theta(\zeta)$ gives $\frac{\partial F}{\partial \theta_i} = \partial_2 F_i(\theta_{i-1}, \theta_i) + \partial_1 F_{i+1}(\theta_i, \theta_{i+1})$,
   so the Hessian, $\nabla^2 F(\boldsymbol{\theta})$, is tridiagonal (assuming ν is given) and is easily inverted.

6. Multi-dimensional Newton method: $\delta\boldsymbol{\theta} = -\left(\nabla^2 F\right)^{-1} \cdot \nabla F(\boldsymbol{\theta})$;
   global integration, <u>much</u> less sensitive to "Lyapunov" integration errors.

The action gradient, ν, is constant along the pseudo fieldlines; construct Quadratic Flux Minimzing (QFM) surfaces by pseudo fieldline (local) integration.

1. The *true* fieldline flow along $\mathbf{B}$ around q toroidal periods from (θ_0, ρ_0) produces a mapping, $\left(\begin{array}{c} \theta_q \\ \rho_q \end{array} \right) = M^q \left(\begin{array}{c} \theta_0 \\ \rho_0 \end{array} \right)$.

2. Periodic fieldlines are fixed points of M^q, i.e. $\theta_q = \theta_0 + 2\pi p, \;\; \rho_q = \rho_0$.

3. In integrable case: given θ_0, a one-dimensional search in ρ is required to find the *true* periodic fieldline.

4. In non-integrable case, only the
   (i) "stable" (action-minimax), O, (which is not always stable), and the
   (ii) unstable (action minimizing), X, periodic fieldlines are guaranteed to survive.

5. The *pseudo* fieldline flow along $\mathbf{B}_\nu = \mathbf{B} - \dfrac{\nu}{\sqrt{g}} \mathbf{e}_\rho$ around q periods from (θ_0, ρ_0) produces a mapping, $\left(\begin{array}{c} \theta_q \\ \rho_q \end{array} \right) = P^q \left(\begin{array}{c} \nu \\ \rho_0 \end{array} \right)$, but ν is not yet known.

6. In general case: given θ_0, a two-dimensional search in (ν, ρ) is required to find the periodic *pseudo* fieldline.

Lagrangian integration is sometimes preferable, but not essential: can iteratively compute radial "error" field

0. Usually, there are only the "stable" periodic fieldline and the unstable periodic fieldline,

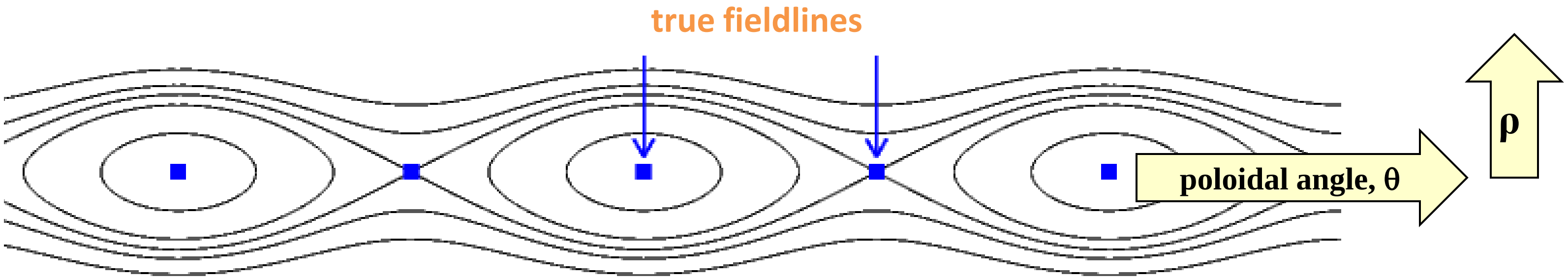

1. At every $\theta = \alpha$, determine $\nu(\alpha)$ via numerical search so that $\mathbf{B} - \nu\, \mathbf{e}_\rho / \sqrt{g}$ yields a periodic integral curve; where α is a fieldline label.

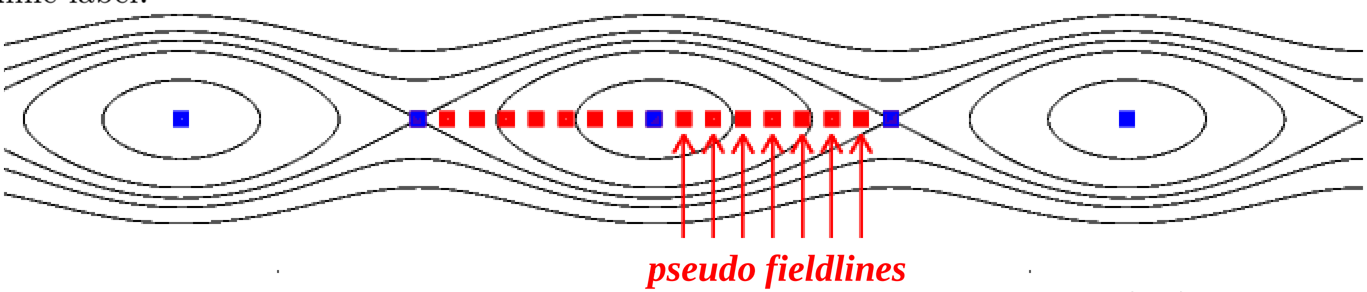

2. At the true periodic fieldlines, the required additional radial field is zero: i.e. $\nu(\alpha_0) = 0$ and $\nu(\alpha_X) = 0$.
3. Typically, $\nu(\alpha) \approx \sin(q\alpha)$.

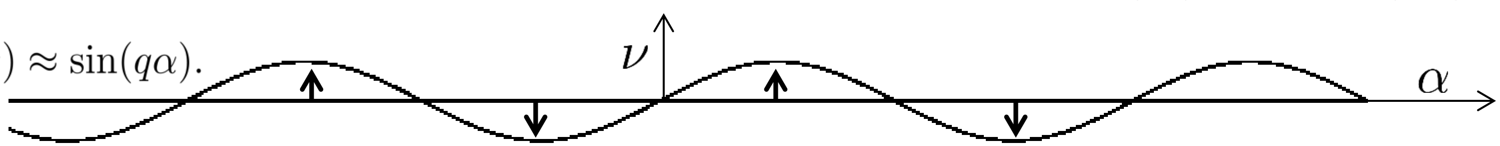

4. The pseudo fieldlines "capture" the true fieldlines; QFM surfaces pass through the islands.

Algorithm
Step 1: start with some magnetic field, in this case provided by M3D-C_1, in cylindrical coordinates . . .

1. Given $\mathbf{B}(R, \phi, Z)$.
2. Given guess, (R_0, Z_0), for magnetic axis on $\phi = 0$ plane
   i. locate magnetic axis by fieldline integration:
      a. follow magnetic field line around $\Delta\phi = 2\pi$
      b. iterate on (R_0, Z_0), until fieldline closes . . .
3. Construct Poincaré plot in cylindrical coordinates.

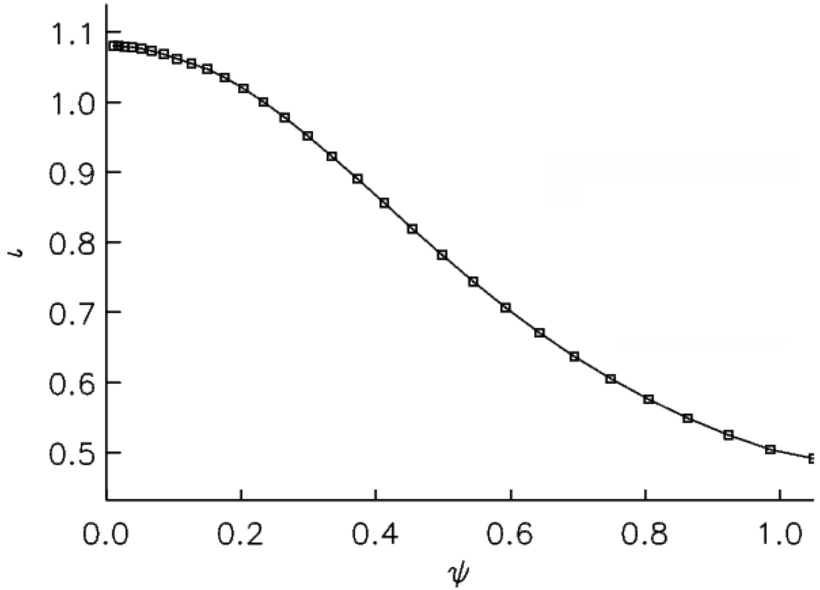

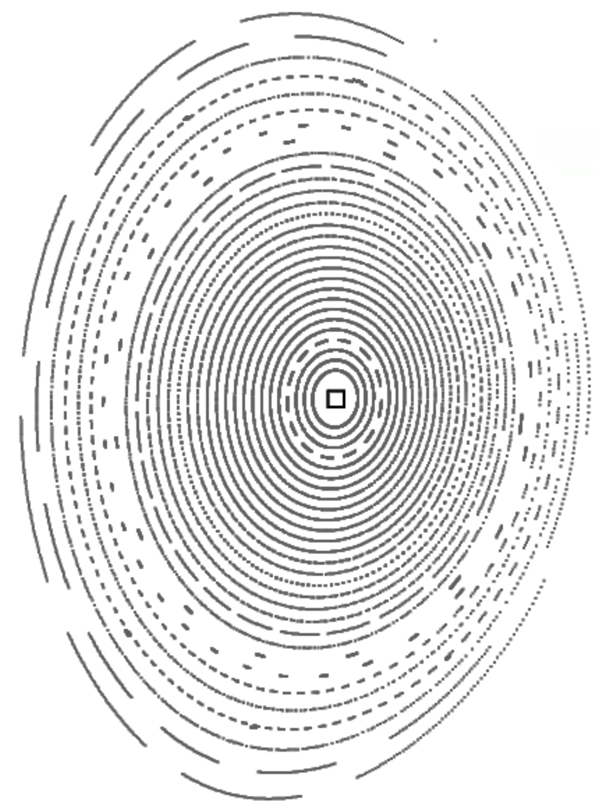

Algorithm
Step 2: construct initial set of toroidal coordinates

1. Unless a better approximation is provided, use circular cross section coordinates based on magnetic axis.

2. Hereafter, will work in toroidal coordinates, (ρ, θ, ζ).

3. The coordinate transformation

$$
\begin{aligned}
R &\equiv R(\rho,\theta,\zeta) = R_0 + \rho\cos\theta \\
\phi &\equiv \zeta \\
Z &\equiv Z(\rho,\theta,\zeta) = Z_0 + \rho\sin\theta
\end{aligned}
$$

   will be iteratively updated to better approximate straight-fieldline flux coordinates, as much as is possible.

4. Construct rotational transform.

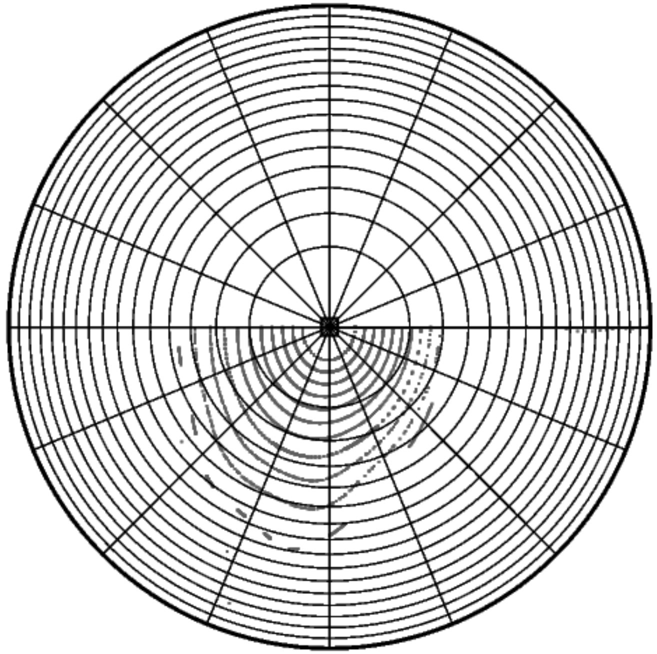

Algorithm
Step 3: construct rational pseudo-surface

1. User must select rational, e.g. $\iota = 1/2$.

2. The cylindrical harmonics of the rational surface are Fourier decomposed in straight *pseudo* fieldline poloidal angle.

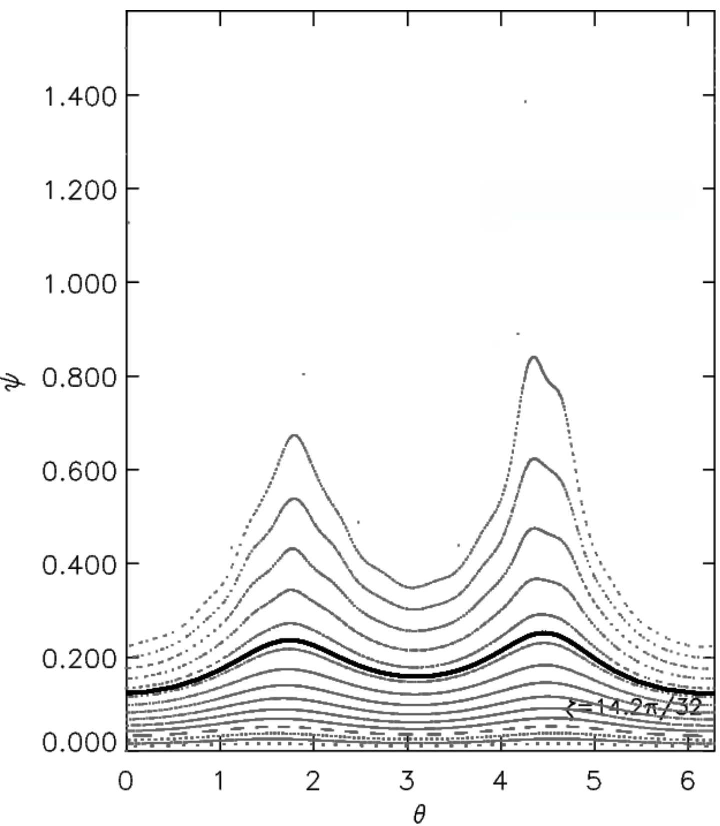

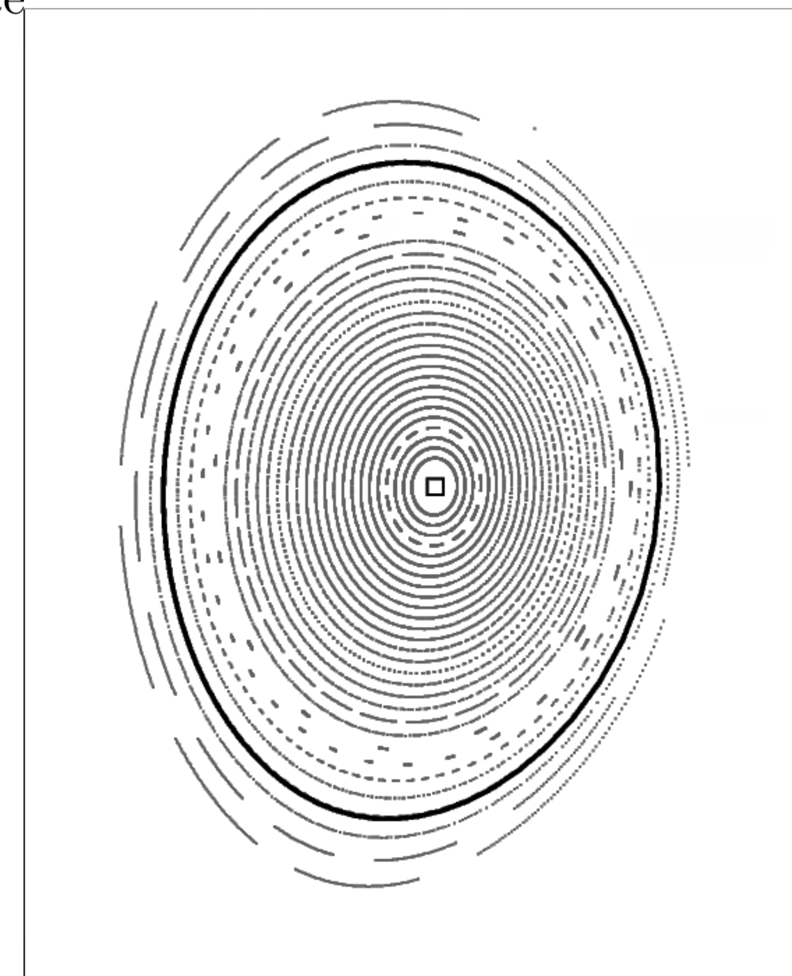

Algorithm
Step 3: update toroidal coordinates

1. The background toroidal coordinates are now based on an interplation/extrapolation of the constructed pseudo surfaces

2. The new coordinates coincide with flux coordinates *only* on the pseudo surfaces.

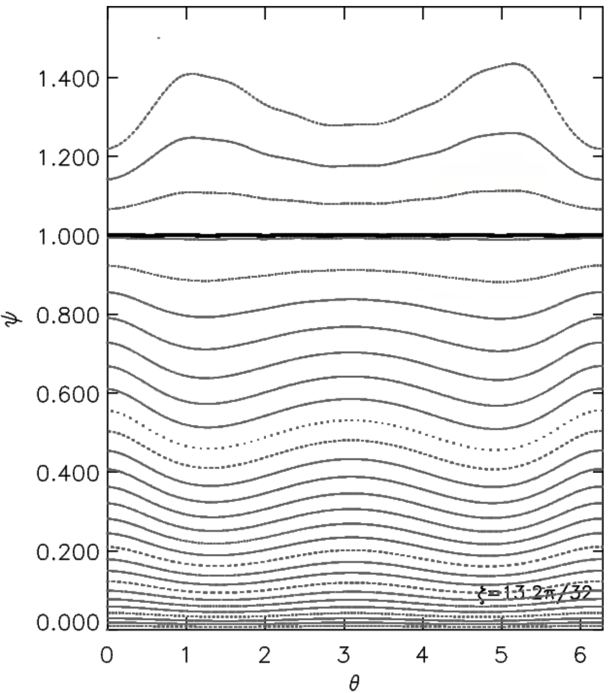

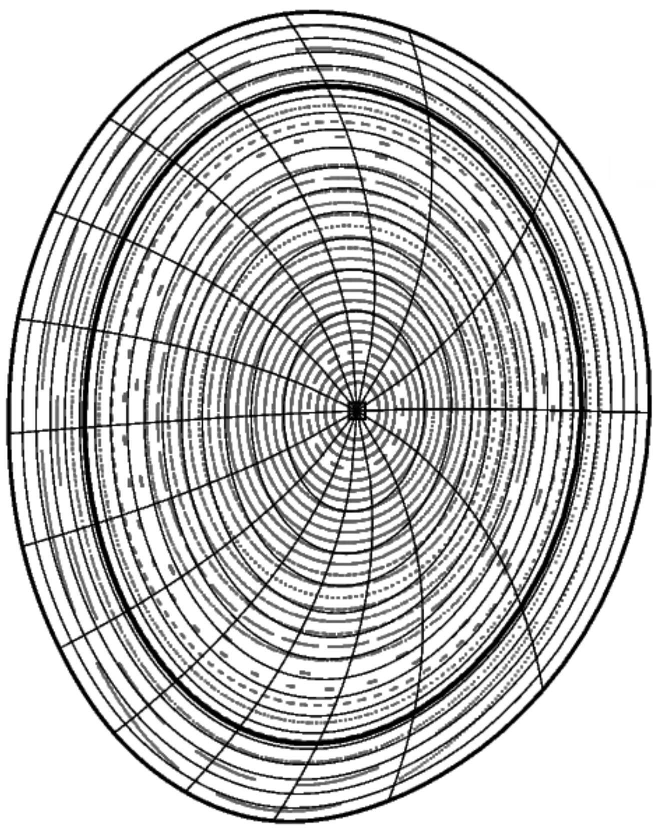

Algorithm
Step 3: repeat:

1. Include additional surfaces.

2. Approximate straight fieldline coordinates.

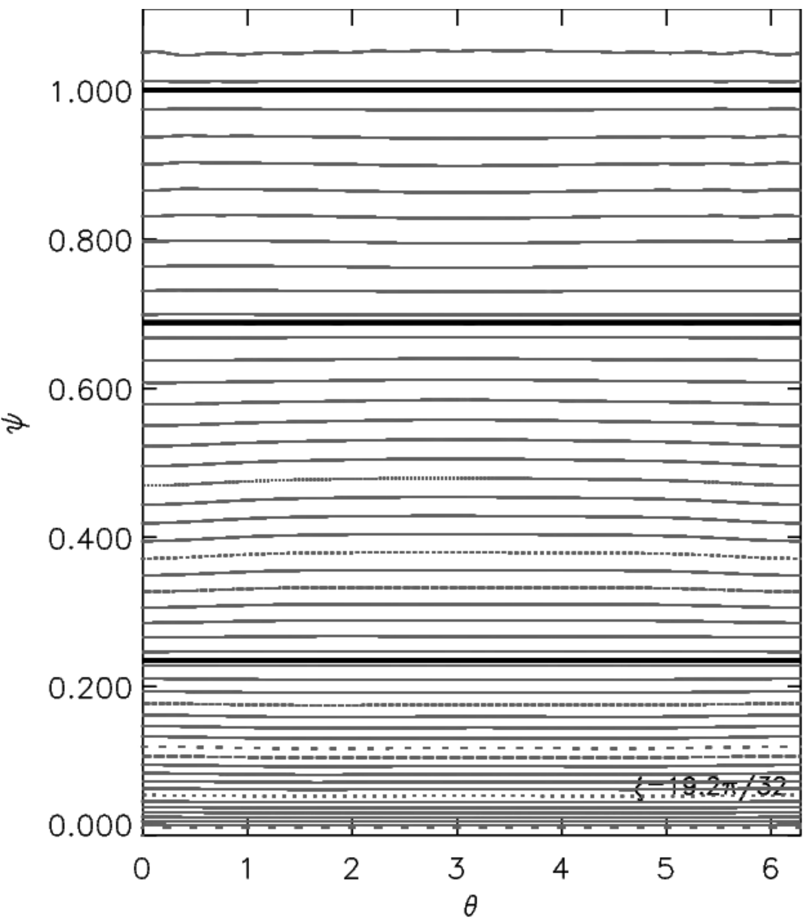

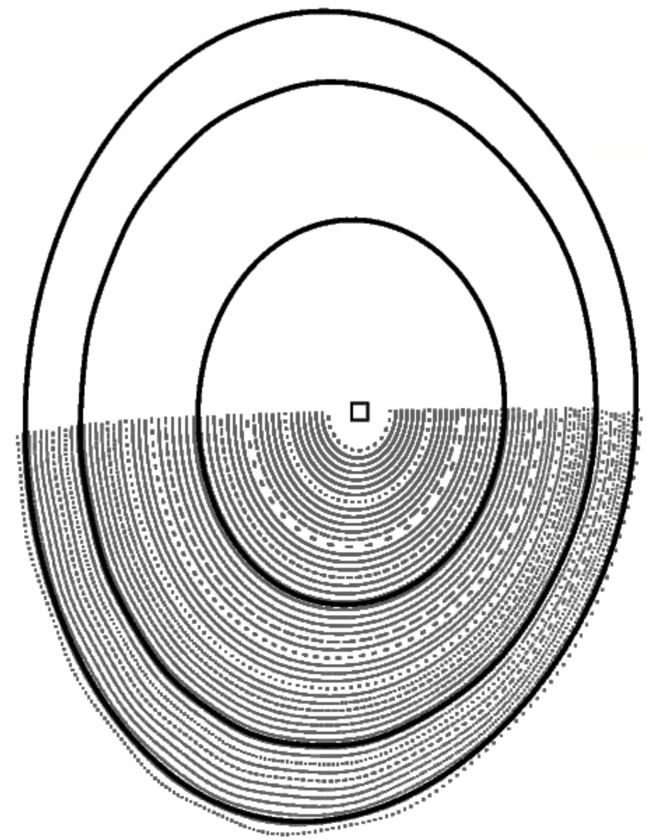

Algorithm
Step 3: repeat:

1. Can examine magnetic field varying in time.

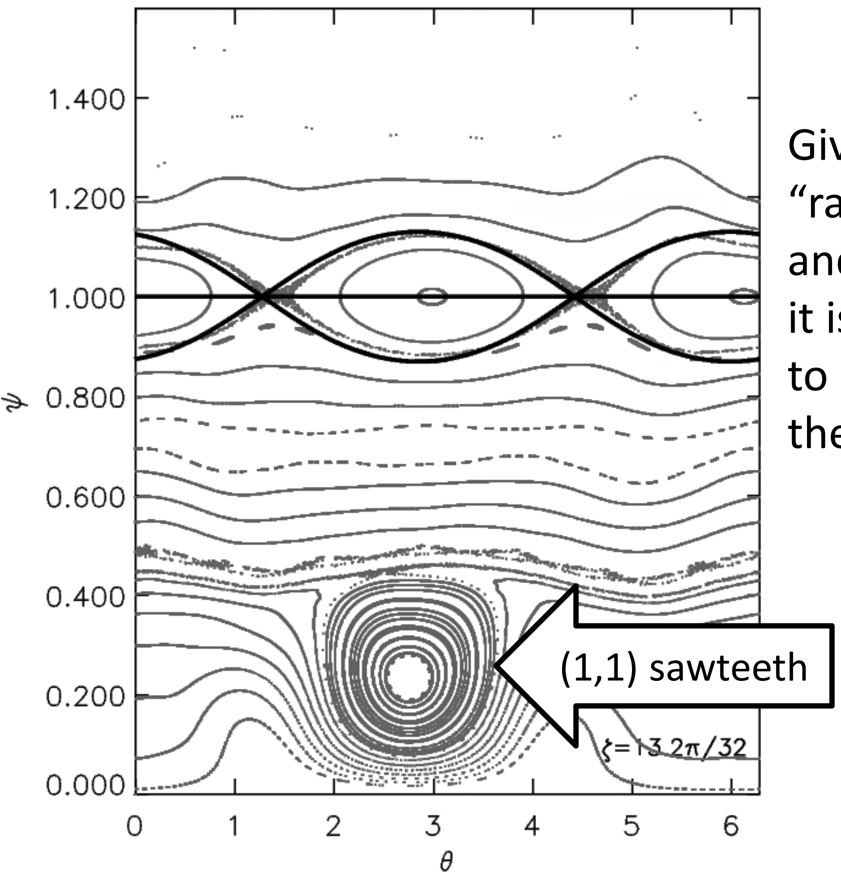

Given the
"rational surface",
and shear,
it is easy
to determine
the island separatrix.

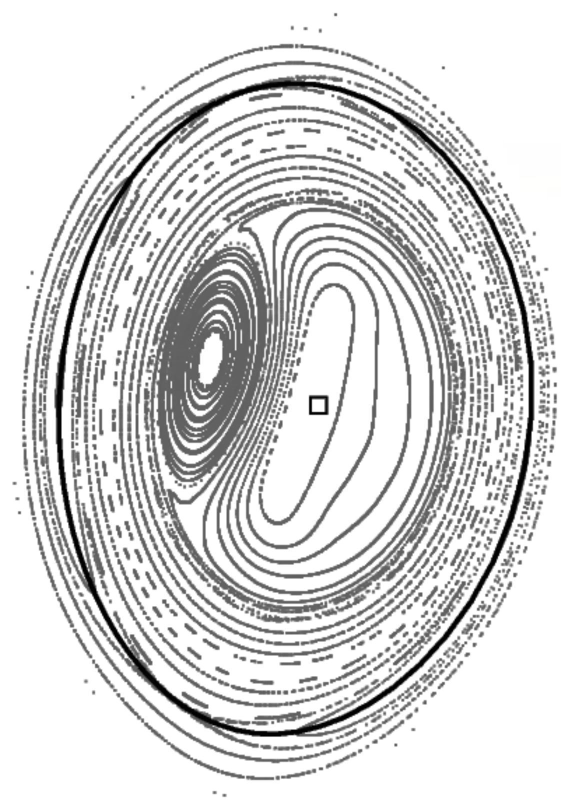

Can also construct separatrix/homoclinic tangle

1. Shown is the

   i. X point;

   ii. the stable and unstable eigenvectors of the tangent map (blue);

   iii. the stable and unstable manifolds;

   iv. the intersections of the stable and unstable manifolds (called the homoclinic points, red squares).

2.

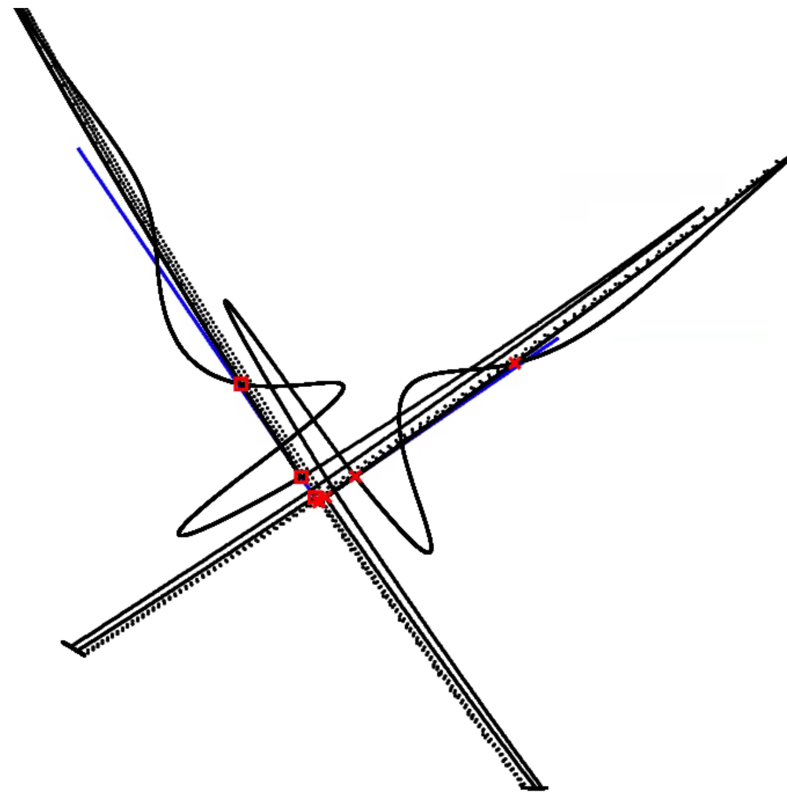

Plan is to construct a flexible library of routines to be made freely available.
(No two users ever seem to want the same thing!)

1. Usually, I like to use the magnetic axis as the coordinate axis, but this has problems when "sawteeth" are present;
   1. coordinate axis = magnetic axis is now a user option.
2. Usually, I like to construct the magnetic vector potential and introduce an almost-straight fieldline angle;
   1. but sometimes it is better to work directly with the cylindrical field provided.
3. The separatrix is a singularity in straight fieldline coordinates;
   1. under construction.
4. Plan is to construct a collection of subroutines that can be used for a variety of purposes;
   1. I plan to visit NIFS this summer and continue to develop these routines . . .

The structure of phase space is related to the structure of rationals and irrationals.

THE FAREY TREE;
or, according to Wikipedia,
THE STERN–BROCOT TREE.

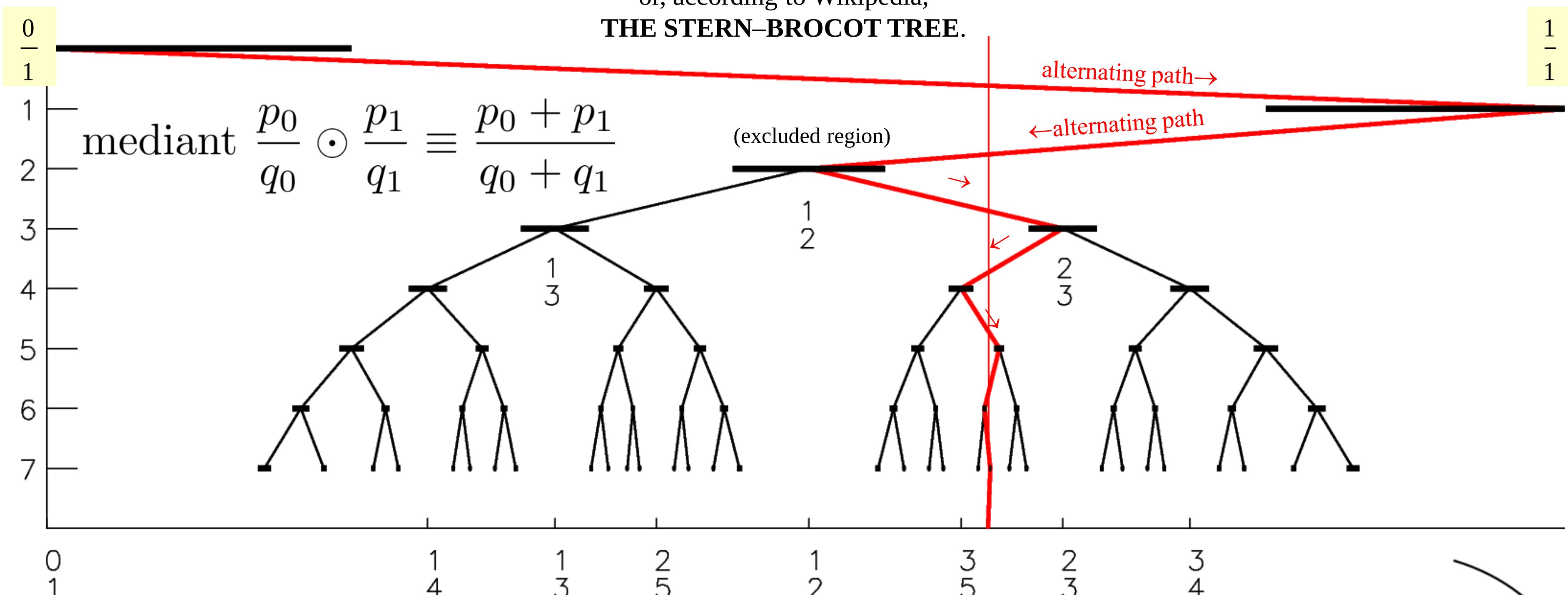

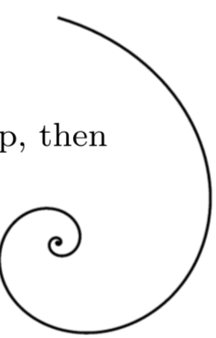

1. Islands, and chaos, emerge at every rational:
   about each rational, n/m, introduce "excluded region" with width r/m^k; if excluded regions don't overlap, then
2. KAM theorem: irrational flux surface can survive if $\underbrace{|\iota - n/m| > r/m^k \text{ for all } n, m.}_{\text{Diophantine condition}}$
   Call ι *strongly irrational.*
3. Greene's residue criterion: the most robust flux surfaces have "noble" transform:
   noble irrationals $\equiv$ limit of ultimately alternating paths $\equiv$ limit of Fibonacci ratios;
   e.g. $\frac{0}{1}, \frac{1}{0}, \frac{1}{1}, \frac{2}{1}, \frac{3}{2}, \frac{5}{3}, \frac{8}{5}, \frac{13}{8}, \frac{21}{13}, \frac{34}{21}, \frac{55}{34}, \dots \to \gamma \equiv$ golden mean $\equiv \frac{(1+\sqrt{5})}{2}$; e.g. $\frac{1}{0}, \frac{0}{1}, \frac{1}{1}, \frac{1}{2}, \frac{2}{3}, \frac{3}{5}, \frac{5}{8}, \frac{8}{13}, \frac{13}{21}, \frac{21}{34}, \dots \to \gamma^{-1}$.

Irrational KAM surfaces break into cantori when perturbation exceeds critical value.
Both KAM surfaces and cantori restrict transport.

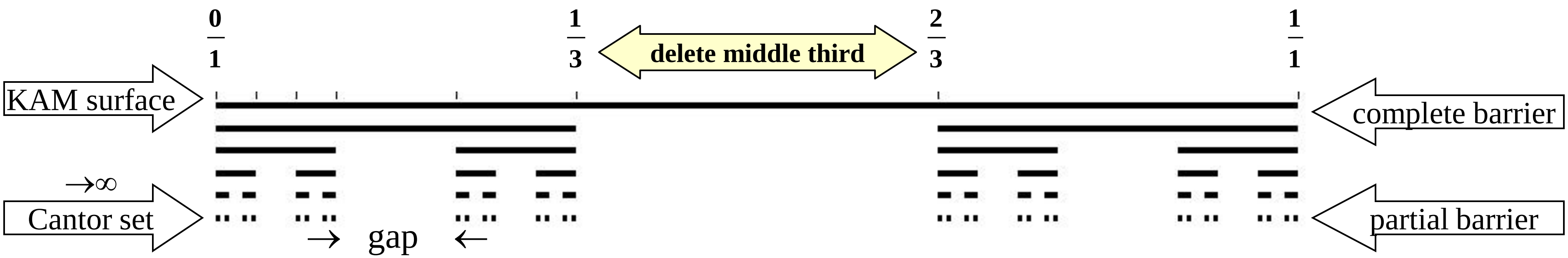

→ KAM surfaces are closed, toroidal surfaces
that **stop** radial field line transport

→ Cantori have "gaps" that fieldlines can pass through;
however, **cantori can severely restrict** radial transport

→ Example: all flux surfaces destroyed by chaos,
but even after **100 000 transits** around torus
the fieldlines **don't get past cantori !**

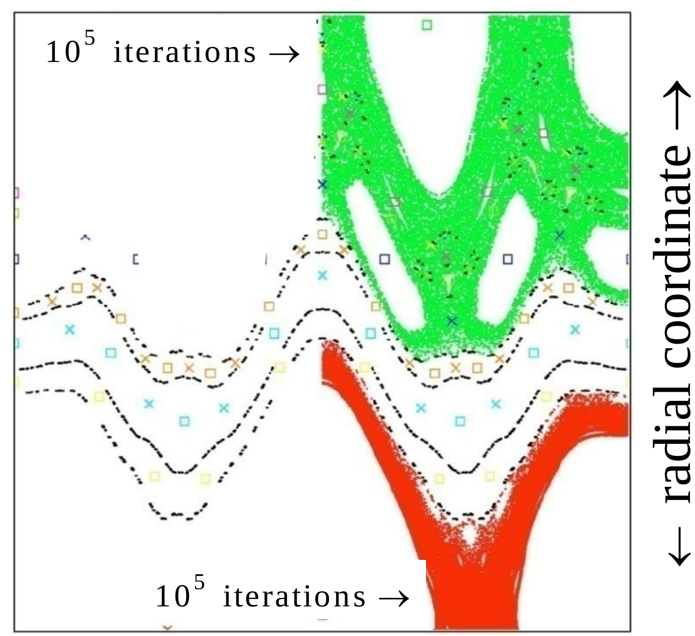

→ Regions of chaotic fields can provide some
confinement because of the cantori partial barriers.

Ghost surfaces are (almost) indistinguishable from QFM surfaces

can redefine poloidal angle to unify ghost surfaces with QFMs.

1. Ghost-surfaces are defined by an (action gradient) flow.
2. QFM surfaces are defined by minimizing $\int (\text{action gradient})^2 d\mathbf{s}$.
3. Not obvious if the different definitions give the same surfaces.
4. For model chaotic field:
   (a) ghosts = thin solid lines;
   (b) QFMs = thick dashed lines;
   (c) agreement is excellent;
   (d) difference = $\mathcal{O}(\epsilon^2)$, where ϵ is perturbation.
5. Can redefine θ to obtain unified theory of ghosts & QFMs; straight *pseudo* fieldline angle.

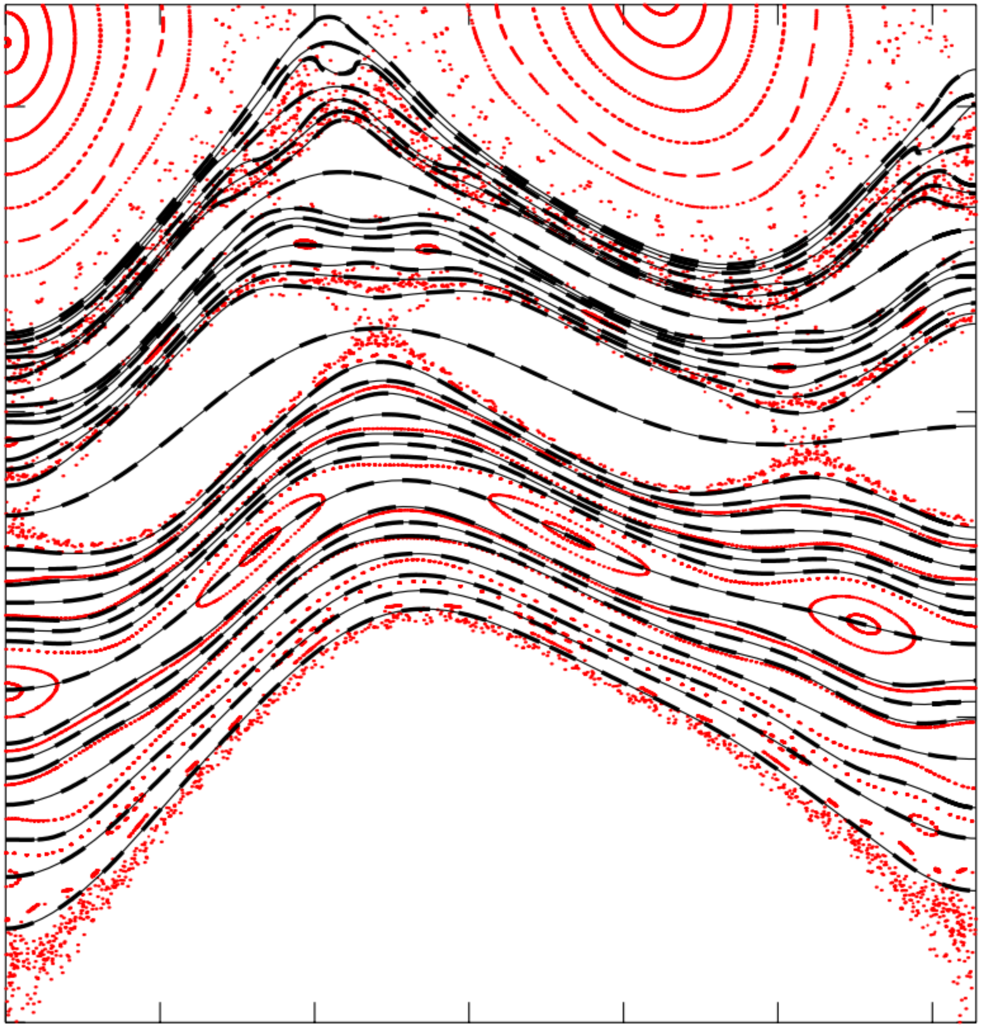

Isotherms of the steady state solution to the anisotropic diffusion coincide with ghost surfaces; analytic, 1-D solution is possible.

1. Transport along the magnetic field is unrestricted:
   e.g. parallel random walk with long steps $\approx$ collisional mean free path.

2. Transport across the magnetic field is very small:
   e.g. perpendicular random walk with short steps $\approx$ Larmor radius.

3. Simple transport model: anisotropic diffusion,
   $\boxed{\kappa_{\parallel}\nabla_{\parallel}^2 T + \kappa_{\perp}\nabla_{\perp}^2 T = 0}$, $\quad \kappa_{\perp}/\kappa_{\parallel} \sim 10^{-10}$, grid $= 2^{12} \times 2^{12}$.
   steady state, no source, inhomogeneous boundary conditions.

4. Compare numerical solution to “irrational” ghost-surfaces

5. The temperature adapts to KAM surfaces, cantori, **and ghost-surfaces!**, i.e. $T = T(\rho)$.

6. From $T = T(\rho, \theta, \zeta)$ to $\boxed{T = T(\rho)}$ allows an expression for the temperature gradient in chaotic fields:

$$\boxed{\frac{dT}{d\rho} \propto \frac{1}{\kappa_{\parallel}\varphi_2 + \kappa_{\perp} G}},$$

where $\varphi_2 \equiv \underbrace{\int B_n^2 \, d\mathbf{s}}_{\text{quadratic flux}}$, and $G \equiv \underbrace{\int \nabla\rho \cdot \nabla\rho \, d\mathbf{s}}_{\text{metric}}$.